

Adsorption of Thiolates to Singly Coordinated Sites on Au(111) Evidenced by Photoelectron Diffraction

H. Kondoh, M. Iwasaki, T. Shimada, K. Amemiya, T. Yokoyama, and T. Ohta*

Department of Chemistry, Graduate School of Science, The University of Tokyo, 7-3-1 Hongo, Bunkyo-ku, Tokyo 113-0033, Japan

M. Shimomura and S. Kono

*Institute of Multidisciplinary Research for Advanced Materials, Tohoku University,
2-1-1 Katahira, Aoba-ku, Sendai 980-8577, Japan*

(Received 24 August 2002; published 10 February 2003)

The adsorption structure of methylthiolate (CH_3S) adsorbed on Au(111), a long-standing controversial issue, has been unambiguously determined by scanned-energy and scanned-angle S $2p$ photoelectron diffraction. The methylthiolate molecules are found to occupy atop sites with a S-Au distance of $2.42 \pm 0.03 \text{ \AA}$. The angular distribution of the S $2p$ photoelectrons due to forward scattering reveals that the S-C bond is inclined by approximately 50° from the surface normal towards both the $[\bar{2}11]$ and $[\bar{1}2\bar{1}]$ (nearest-neighbor thiolate) directions.

DOI: 10.1103/PhysRevLett.90.066102

PACS numbers: 68.43.Fg, 68.49.Jk, 81.16.Dn

Self-assembled monolayers (SAMs) of alkanethiols on Au(111) are the prototypical SAM system, and their structure and growth have been extensively studied with many surface-science techniques [1]. Although a consensus of the molecular-level picture for the growth mechanism has already emerged [2,3], the structure of the alkanethiol SAMs on Au(111), particularly the structure at the molecule/substrate interface, has been controversial both from the experimental and the theoretical points of view [4–16].

In the early years it was usually assumed that alkanethiol molecules are dissociatively adsorbed in the form of Au-thiolate at threefold hollow sites on the (111) surface of gold. This picture has been first challenged by grazing-incidence x-ray diffraction study [4], where it was proposed that the surface thiolates form dimers and adsorb as disulfides. Although this model was supported by subsequent studies using sum frequency generation [5], temperature programmed desorption [6], and x-ray standing wave (XSW) method [7], a high-resolution energy loss spectroscopy study [8] reported that the disulfidelike surface complex is not formed at room temperature (RT) but at an elevated surface temperature (375 K).

As for the theoretical side, recent density functional theory (DFT) studies on $\text{CH}_3\text{S}/\text{Au}(111)$, which is the simplest alkanthiolate/Au adsorption system, reached two different conclusions; Grönbeck *et al.* [9] and Yourdshahyan *et al.* [10] concluded that the fcc-hollow site is energetically the most favorable one and that the S-C bond is aligned along the surface normal, while Morikawa *et al.* [11,12] found that methylthiolate is bound at the bridgelike position, which is shifted from the regular bridge position slightly toward the fcc-hollow site (hereafter denoted by the fcc-bridge site) as shown in Fig. 1, with the S-C bond significantly tilted from the surface normal. The latter finding was further supported

by subsequent DFT calculations using a Au(111) cluster [13] and a slab [14]. Very recently, a STM study on cysteine-adsorbed Au(110) revealed the existence of a significant amount of surface vacancies, and it has been proposed from DFT calculations that the S atoms of cysteine sit at bridgelike sites on the defected surface [15]. In connection to this study, the latest theoretical work claims that the methylthiolate SAM on Au(111) is also stabilized by a vacancy structure in the first Au layer [16]. However, several theoretical groups have recently pointed out that current DFT calculations do not always give correct structural predictions particularly for adsorbates on noble-metal surfaces [17]. It is strongly desirable to determine the adsorption structure of the thiolate on Au(111) *experimentally*.

In this Letter we report the structure of CH_3S adsorbed on a Au(111) single crystal surface unambiguously determined by scanned-energy and scanned-angle photoelectron diffraction (PD) [18]. Contrary to the above theoretical predictions, the results of the two PD mode measurements indicate that CH_3S is located at the atop

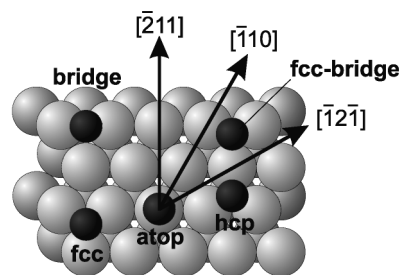


FIG. 1. Schematic illustration for high-symmetry sites on the unreconstructed (111) surface of Au. The fcc-bridge site that is considered to be energetically most stable according to the recent theoretical studies [11–14] is also indicated.

position of the defect-free Au(111) surface. It is also found that the S-C bond is considerably bent from the surface normal.

The PD experiments were carried out at the beam line 7A in the Photon Factory [19]. The end station at this beam line is equipped with a hemispherical analyzer (GAMMADATA-SCIENIA SES-2002) for collection of photoelectron spectra, along with a five-axes sample manipulator. A Au(111) single crystal surface was cleaned by repeated cycles of Ar ion bombardment and annealing at 820 K. The crystal axes of the Au(111) surface were determined by low-energy electron diffraction (LEED) and scanned-angle photoelectron diffraction. Methylthiolate monolayers were prepared by exposing the clean Au(111) surface to the vapor of dimethyldisulfide (CH_3SSCH_3) at RT, which is dissociatively adsorbed on Au(111) as methylthiolate [11]. Saturated methylthiolate monolayers on Au(111) gave $(\sqrt{3} \times \sqrt{3})R30^\circ$ LEED pattern which disappears within 60 s. High-resolution S $2p$ photoelectron spectra for the methylthiolate monolayers without electron-beam irradiation exhibited a single spin-orbit component at 161.9 and 163.1 eV for $2p_{3/2}$ and $2p_{1/2}$, respectively. It was carefully confirmed that no x-ray-induced decomposition took place after each scan [20]. Scanned-energy data were collected over the photon energy range of 190–550 eV ($k_{S2p} = 2.8\text{--}10.1 \text{ \AA}^{-1}$) for several polar and azimuthal emission angles. The angular acceptance of the analyzer is $\pm 5^\circ$. Scanned-angle data were obtained over the polar angle range of $\theta = 0\text{--}85^\circ$ from the surface normal along the major three azimuths, $[\bar{2}11]$, $[\bar{1}10]$, and $[\bar{1}2\bar{1}]$ as indicated in Fig. 1. All the data sets were acquired at RT without any annealing. Each S $2p$ intensity was normalized with the photon intensity for the scanned-energy data and with the C $1s$ intensity for the scanned-angle data, respectively. The diffraction modulation function was extracted from the intensity-energy and intensity-angle spectra using the χ function, defined as $\chi = (I - I_0)/I_0$, where I and I_0 are the diffractive and nondiffractive intensities [18].

Figure 2(a) shows scanned-energy PD modulation functions taken at several emission directions for a saturated methylthiolate monolayer formed on Au(111) at RT. The normal-emission function exhibits strong oscillations with almost a single period, while the grazing-emission functions show significant decrease of the oscillation amplitudes. Since single-period strong oscillations are characteristic of a 180° scattering from a near neighbor [18], such angular dependence suggests existence of a Au atom beneath the S atom of the thiolate. This is further supported by comparison between the experimental functions and theoretical simulations. The simulations were performed using the multiple scattering calculation of diffraction (MSCD) package developed by Chen and van Hove [21], which is based on the spherical-wave multiple-scattering theory. A cluster with more than 200 atoms was used to model the adsorption geometry.

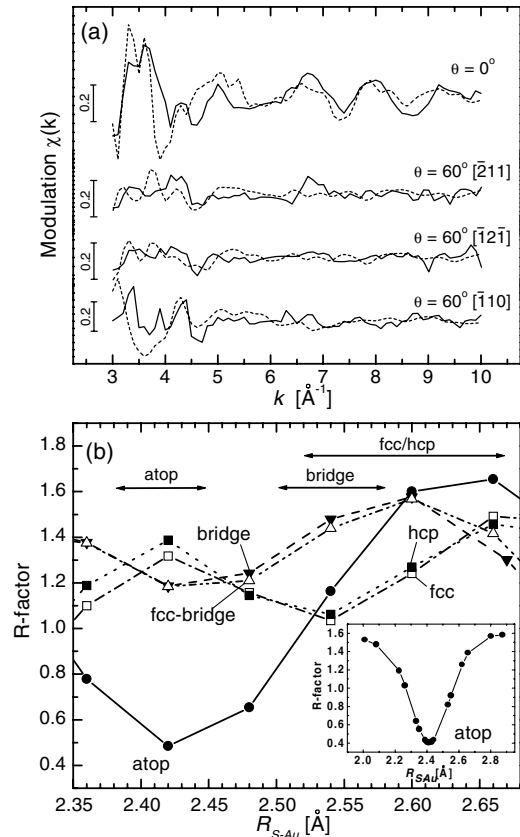


FIG. 2. (a) Solid curves: scanned-energy S $2p$ PD modulation functions $\chi(k)$ s recorded in different emission directions for a saturated CH_3S monolayer adsorbed on Au(111) at room temperature. Dashed curves: theoretical simulations for the best-fit atop adsorption model. (b) k^2 -weighted R factors of the simulations for the normal-emission curve as a function of the S-Au distance. Simulations are for the $(\sqrt{3} \times \sqrt{3})R30^\circ$ -S adlayer on Au(111) at five possible adsorption sites. Inset: R -factor change for a $(\sqrt{3} \times \sqrt{3})R30^\circ$ - CH_3S structure bonding to the atop site with the S-C axis tilted by 50° from the surface normal and aligned along $[\bar{2}11]$ azimuth (see text) as a function of the S-Au distance. Horizontal arrows at the top indicate the possible range of S-Au distance for each site obtained from geometrical optimization in the previous DFT studies [11–14].

Based on the LEED observation, the $(\sqrt{3} \times \sqrt{3})R30^\circ$ periodicity was assumed for the two-dimensional arrangement of methylthiolate in all the simulations. We have investigated the optimum S-Au distance for each site through the R -factor analyses [18] for the normal-emission data. Since the difference between the simulated functions with and without the carbon moiety is fairly small, carbonless models were used for a rough survey for the optimum S-Au distance. Variation of the k^2 -weighted R factor for each site is shown as a function of the S-Au distance in Fig. 2(b). Obviously, only the atop model presents a clear minimum of the R factor at 2.42 Å, while the other models give no apparent minimum. In the inset is shown the R -factor change obtained by simulations for a carbon-including atop model where the S-C bond axes are tilted by 50° from the surface normal and

aligned along $[\bar{2}11]$ azimuth. The direction of the S-C axes was deduced from the scanned-angle experiments described below. The R -factor minimum was further lowered by including the C atom and found at $2.42 \pm 0.03 \text{ \AA}$ again. These results provide firm evidence for the atop adsorption contrary to the previous DFT studies where the atop site is energetically the most unfavorable [11–14]. This atop model gives the best fit to all the scanned-energy PD modulation functions as shown in Fig. 2(a) (dashed curves).

Scanned-angle PD data were taken at a wave number of 9 \AA^{-1} , where photoelectron diffraction is dominated by the forward scattering by the carbon atoms [18]. From the data recorded at the forward-scattering mode the orientation of the S-C bond is elucidated. Figure 3(a) shows S $2p$ intensity change as a function of polar emission angle (θ) taken at $k = 9 \text{ \AA}^{-1}$ in the planes along $[\bar{2}11]$, $[\bar{1}2\bar{1}]$, and $[\bar{1}10]$ azimuths. Each S $2p$ intensity is normalized by the corresponding C $1s$ intensity. Although the signal to noise ratio is relatively poor due to the high wave number used here, the angle dependence taken for $[\bar{2}11]$ and $[\bar{1}2\bar{1}]$

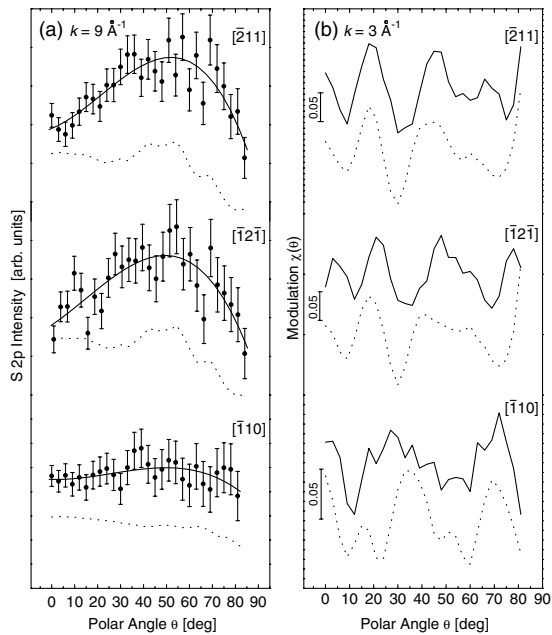


FIG. 3. Scanned-angle S $2p$ PD data for a CH_3S monolayer saturated on Au(111) at room temperature. (a) Polar angle (θ) dependence of the S $2p$ intensity normalized by the C $1s$ one (solid circles) at a wave number of $k = 9 \text{ \AA}^{-1}$ recorded along three different azimuths, $[\bar{2}11]$, $[\bar{1}2\bar{1}]$, and $[\bar{1}10]$. Solid lines are guides for the eye. Dashed lines show multiple scattering simulations for atop CH_3S structures with the S-Au distance of 2.42 \AA and with the S-C axes tilted by 50° from the surface normal and aligned along $[\bar{2}11]$, $[\bar{1}2\bar{1}]$, and their symmetrically equivalent four azimuths. (b) Scanned-angle PD modulation functions $\chi(\theta)s$ (solid line) at a wave number of $k = 3 \text{ \AA}^{-1}$ recorded along the three different azimuths. Simulated modulation functions are shown as dashed lines for the same geometries as used in the left panel but at $k = 3 \text{ \AA}^{-1}$.

azimuths, i.e., the nearest-neighbor (NN) direction of the $(\sqrt{3} \times \sqrt{3})R30^\circ$ lattice, exhibits a broad peak centered at around 50° . On the other hand, no apparent peak is observed for the $[\bar{1}10]$ azimuth, i.e., second-nearest-neighbor direction. This clear difference in angle dependence leads us to conclude that the S-C bond of the methylthiolate prefers tilting towards the NN directions. Dashed lines in Fig. 3(a) are results of the simulations assuming that the S-C bond is tilted by 50° from the surface normal along $[\bar{2}11]$, $[\bar{1}2\bar{1}]$, and their symmetrically equivalent four azimuths. It is confirmed from the simulation that the tilting towards the NN directions causes no prominent peak along the $[\bar{1}10]$ azimuth. The observed angle dependences for the $\langle 211 \rangle$ azimuths are broader than the simulated ones. This suggests that the S-C tilt angle has a static and/or dynamic distribution in the plane perpendicular to the surface at RT. In fact, the previous STM observations of methylthiolate monolayers formed on Au(111) at RT revealed significant molecular motion faster than the scanning rate of STM tips [22], supporting the dynamic distribution of the tilt angle.

In Fig. 3(b) is depicted scanned-angle modulation functions $\chi(\theta)s$ recorded along the three azimuths at $k = 3 \text{ \AA}^{-1}$ where backward scattering from Au atoms dominantly contributes to diffraction. This gives information about the adsorption site. R -factor analyses for the $\chi(\theta)$ functions were performed to determine the most favorable site, and the results are listed in Table I. As evidenced in the comparison of the R factors, the atop site model gives the best fit to the experimental results again. Simulated $\chi(\theta)$ functions using the atop site model are shown as dashed lines in Fig. 3(b). Both of the scanned-energy and scanned-angle PD analyses for the methylthiolate monolayers indicate that the atop site is the most probable site. A structure model thus determined by the present PD analyses is shown in Fig. 4. The methylthiolate molecules are bound to the atop sites with the S-Au distance of $2.42 \pm 0.03 \text{ \AA}$ and with the S-C bond axes tilted by approximately 50° from the surface normal towards the $\langle 211 \rangle$ (NN) directions. It should be noted that in the previous XSW study on the structure of a C10-thiolate/Au(111) system Fenter *et al.* proposed the asymmetric dimer model in which one of the two sulfur head groups is located at the atop site with a vertical height of 2.21 \AA and the other one at the fcc-hollow site with 2.97 \AA [7]. From the large difference in vertical

TABLE I. R factors for the best fit to the $\chi(\theta)$ functions from the scanned-angle data obtained for three azimuths with a fixed wave number of photoelectron of $k = 3 \text{ \AA}^{-1}$.

	fcc	hcp	Bridge	Atop
$[\bar{2}11]$	0.507	0.712	0.837	0.185
$[\bar{1}2\bar{1}]$	0.946	1.334	0.524	0.547
$[\bar{1}10]$	0.962	1.394	1.264	0.400
Average	0.805	1.147	0.875	0.377

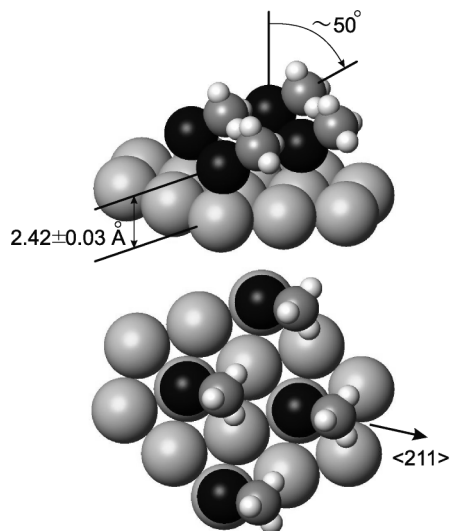


FIG. 4. Schematic side and top view of the best-fit adsorption geometry of $(\sqrt{3} \times \sqrt{3})R30^\circ$ -CH₃S on Au(111). The hydrogen atoms are indicated at tentatively assumed positions.

height between the two sulfur atoms they considered that the dimer is bound primarily through only the atop sulfur atom, which is consistent with the present result. Although we carefully investigated the dimer model [7], evidence for the sulfur pairing was not found, at least in the present system.

Very recently the STM study on a thiolate adsorbed on Au(110) revealed that the thiolate adsorption causes regular vacancies in the first Au layer [15]. The subsequent DFT study of CH₃S-induced vacancy on Au(111) found that adsorption of CH₃S at low-coordination sites on the $(\sqrt{3} \times \sqrt{3})R30^\circ$ vacancy structures in the topmost Au layer is energetically more stable with respect to the best model (fcc-bridge model) on the perfect Au(111) surface [16]. Simulated $\chi(k)$ functions for the vacancy models were compared with the present experimental results, but the predicted structures do not reproduce the experimental functions. Furthermore, preliminary STM observation for a CH₃S-covered Au(111) surface confirmed that the topmost Au layer consists of a defect-free (1×1) hexagonal lattice [23]. Thus the defect models are excluded.

In conclusion, we have determined by PD the structure of CH₃S molecules adsorbed on Au(111), which has been under controversy, and found that they are adsorbed at the singly coordinated sites with their molecular axes significantly tilted from the surface normal towards $\langle 211 \rangle$ azimuths. Although the comparability of this result with long-chain thiols is limited due to difference in intermolecular interactions, the present study contributes to the fundamental understanding of the Au-thiolate bond. Detailed molecular-level measurements of the nature of the binding of organic molecules to metallic surfaces, such as those described in this Letter, may become

important to the development of molecular electronic devices.

We thank Dr. Yositada Morikawa, Dr. Luis M. Molina, and Dr. Bjørk Hammer for providing their preprints and the coordinates of the structure models optimized by the DFT calculations and for stimulating discussion. We are grateful for the financial support of Grant-in-Aids for scientific research (No. 14204069). The present work has been performed under the approval of the Photon Factory Program Advisory Committee (PF PAC No. 01S2003).

*Corresponding author.

Email address: ohta@chem.s.u-tokyo.ac.jp

- [1] F. Schreiber, Prog. Surf. Sci. **65**, 151 (2000).
- [2] G. E. Poirier and E. D. Pylant, Science **272**, 1145 (1996).
- [3] H. Kondoh, C. Kodama, H. Sumida, and H. Nozoye, J. Chem. Phys. **111**, 1175 (1999).
- [4] P. Fenter, A. Eberhardt, and P. Eisenberger, Science **266**, 1216 (1996).
- [5] M. S. Yeganeh, S. M. Dougal, R. S. Polizzotti, and P. Rabinowitz, Phys. Rev. Lett. **74**, 1811 (1995).
- [6] N. Nishida, M. Hara, H. Sasabe, and W. Knoll, Jpn. J. Appl. Phys. **35**, 5866 (1996).
- [7] P. Fenter, F. Schreiber, L. Berman, G. Scoles, P. Eisenberger, and M. J. Bedzyk, Surf. Sci. **412/413**, 213 (1998).
- [8] G. J. Kluth, C. Carraro, and R. Maboudian, Phys. Rev. B **59**, 10 449 (1999).
- [9] H. Grönbeck, A. Curioni, and W. Anderoni, J. Am. Chem. Soc. **122**, 3839 (2000).
- [10] Y. Yourdshahyan, H. K. Zhang, and A. M. Rappe, Phys. Rev. B **63**, 081405 (2001).
- [11] T. Hayashi, Y. Morikawa, and H. Nozoye, J. Chem. Phys. **114**, 7615 (2001).
- [12] Y. Morikawa, T. Hayashi, C. C. Liew, and H. Nozoye, Surf. Sci. **507–510**, 46 (2002).
- [13] Y. Akinaga, T. Nakajima, and K. Hirao, J. Chem. Phys. **114**, 8555 (2001).
- [14] J. Gottschalck and B. Hammer, J. Chem. Phys. **116**, 784 (2002).
- [15] A. Kühnle, T. R. Linderoth, B. Hammer, and F. Besenbacher, Nature (London) **415**, 891 (2002).
- [16] L. M. Molina and B. Hammer, Chem. Phys. Lett. **360**, 264 (2002).
- [17] P. J. Feibelman, B. Hammer, J. K. Nørskov, F. Wagner, M. Scheffler, R. Stumpf, R. Watwe, and J. Dumesic, J. Phys. Chem. B **105**, 4018 (2001).
- [18] D. P. Woodruff and A. M. Bradshaw, Rep. Prog. Phys. **57**, 1024 (1994).
- [19] K. Amemiya, H. Kondoh, T. Yokoyama, and T. Ohta, J. Electron Spectrosc. Relat. Phenom. **124**, 151 (2002).
- [20] K. Heister, M. Zharnikov, M. Grunze, L. S. O. Johansson, and A. Ulman, Langmuir **17**, 8 (2001).
- [21] Y. Chen and M. A. van Hove, MSCD package, Lawrence Berkeley National Laboratory (1998).
- [22] H. Kondoh and H. Nozoye, J. Phys. Chem. B **103**, 2585 (1999).
- [23] H. Kondoh and H. Nozoye (unpublished).